

Research paper

The soil bacterial communities show resilience in composition and function for 30 years of pine self-reforestation on agricultural lands in Western Russia

Olga V. Shopina^{a,b}, Aleksey I. Bondar^b, Elena V. Tikhonova^a, Anastasiya V. Titovets^c, Ivan N. Semenkov^{a,b,*}

^a Center for Forest Ecology and Productivity of the Russian Academy of Sciences, Moscow 117997, Russian Federation

^b Lomonosov Moscow State University, Moscow 119234, Russian Federation

^c Institute of Forest Science, Russian Academy of Sciences, Uspenskoe 143030, Russian Federation

ARTICLE INFO

Keywords:

Boreal forests
Environmental gradient
Environmental filtering
Fallow
Space-for-time substitution

ABSTRACT

The taxonomic and functional composition of the soil microbiome plays a crucial role in diverse ecosystem services including the carbon cycle and fertility, and is intricately linked to environmental conditions. Agricultural land abandonment followed by ecosystem changes and reforestation is widely spread in Eastern Europe and especially in Russia where up to 400,000 km² have been extracted from agricultural land-use and started to self-reforest. In boreal ecosystems, the reuse of abandoned lands for agriculture reduces the environmental risk connected with climate change. Therefore, there is a need to assess changes in soil parameters during long-term abandonment. This research aims to investigate the effect of natural pine reforestation on poor sandy ploughing lands on the taxonomic and functional composition of soil bacteria in Smolenskoe Poozerye National Park (western Russia). The soil microbial community of early stages (<30 years of pine reforestation) and older stages (>70 years of pine reforestation) differ significantly ($p < 0.05$): relative abundance of the dominant soil bacteria namely Acidobacteriota (13 % → 21 %), RCP2-54 (0.3 % → 6 %), Verrucomicrobiota (0.8 % → 0.9 %), Dependientiae (0.1 % → 0.7 %), WPS-2 (0.1 % → 1.2 %) increased, while the abundance of Actinobacteriota (24 % → 18 %), Chloroflexi (7 % → 0.7 %), Gemmatimonadota (2.8 % → 0.6 %), Myxococcota (3.2 % → 1.6 %), Bacteroidota (4.6 % → 1.5 %), Latescibacterota (0.1 % → 0 %), Nitrospirota (0.3 % → 0.01 %; $p < 0.05$) decreased. In the 0–30 cm topsoil humus horizon, the younger forest soil microbiome was more similar to soils of meadows and agroecosystems than to the older forests due to previous plough. Differences between the upper and lower parts of the previously homogenized ploughed horizon become more evident during pine reforestation. In terms of predicted metabolic pathways, the younger soil microbiome produces siderophores and degrades organic substances more actively ($p < 0.05$). Older forest communities show higher activity of fermentation, photosynthesis, non-organic nutrient assimilation and respiration ($p < 0.05$). Our results also suggest that reforestation of poor sandy soils is not always beneficial for soil bacteria, since alpha-diversity decreases during succession and certain taxa are more abundant in soils of ploughing lands and native forests than at the transitional stages. The ploughing effect is preserved in soils studied for at least 30 years. The results obtained can be used in the environmental assessment to evaluate the degree and rate of restoration of soils in impacted areas.

1. Introduction

Agricultural land abandonment and consequent reforestation affect vast territories worldwide. In Russia, up to 400,000 km² have been extracted from agricultural land-use and started to self-reforest (Lyuri et al., 2010). This process affects soil by altering environmental

conditions and removing anthropogenic impacts, leading to significant changes in various soil properties (Daskalova and Kamp, 2023). In particular, the composition and diversity of microbial communities undergo notable transformations.

Soil ecosystem services, such as nutrient cycling and organic matter decomposition, are largely defined by bacterial communities (Baldrian

* Corresponding author at: Lomonosov Moscow State University, Moscow 119234, Russian Federation.

E-mail address: semenkov@geogr.msu.ru (I.N. Semenkov).

<https://doi.org/10.1016/j.apsoil.2024.105570>

Received 24 May 2024; Received in revised form 21 July 2024; Accepted 2 August 2024

0929-1393/© 2024 Elsevier B.V. All rights are reserved, including those for text and data mining, AI training, and similar technologies.

et al., 2023; Bereczki et al., 2024). Post-agricultural succession greatly alters soil microbiome composition, and its functions (Gschwend et al., 2022; Lan et al., 2022). The state of the soil bacterial community can therefore serve as a key indicator of ecosystem restoration (Abakumov et al., 2023; Lavrishchev et al., 2024; Wu et al., 2024). This is particularly important in terms of re-engaging abandoned soils in agricultural practices, carbon sequestration management and climate change mitigation.

Forest succession influence on the soil microbiome is well studied in tropical forests (Chernov et al., 2021; Merloti et al., 2019) and temperate forests of China, Europe and the USA (Zhou et al., 2017). Similar studies conducted in the hemiboreal zone of Russia are rare (Abakumov et al., 2023). Only fragmentary data are available on the microbiome of Russian agricultural soils (Kaiser et al., 2016; Semenov et al., 2023; Zverev et al., 2021). However, soils formed in the territory of the last glaciation, as the youngest on the East European Plain, can provide a unique and informative model for understanding ecosystem restoration processes.

Despite extensive research on the soil microbiome, several crucial questions remain unanswered: 1. How long does it take for the soil microbiome of ploughed lands to recover to a state resembling that of old-growth boreal forests? 2. Is there a pattern of succession in the microbial community during natural reforestation observed for soils and vegetation? 3. How persistent is the composition of microbial communities formed on arable lands? 4. Which soil bacteria representatives demonstrate the greatest sensitivity or resilience to environmental changes during natural regeneration processes?

The main prehypothesis for this study was 'soil microbiome formed in croplands due to adverse agricultural activity (ploughing, liming, aeration, entering manure and mineral fertilizers) is recovering during pine reforestation'. The following hypotheses were tested: i. reforestation enhances bacterial diversity by reducing the impacts of fertilization and intensifying resource competition, thereby altering the predicted metabolic pathways provided by soil microbiota; ii. deeper soil horizons are less influenced by these dynamics. To test these hypotheses, the following questions were addressed: (1) What are the primary differences in the structure and composition of microbial communities across various soil layers? (2) How does bacterial composition vary with forest succession age? (3) What are the effects of microbial community changes on the abundance and composition of predicted metabolic pathways?"

2. Materials and methods

2.1. Site description

In this research, the impact of natural pine reforestation was investigated on the soil microbiome and bacterial metabolic pathways composition in poor sandy ploughing lands of Smolenskoe Poozerye National Park, hemiboreal zone of the central part of the East-European plain (Ahti et al., 1968). Here, natural pine forests of diverse ages grow on abandoned ploughing lands and non-ploughed areas (Shopina et al., 2023; Terekhova et al., 2023). The climate of the region is humid continental (Dfb – Köppen classification). An average January air temperature is -4.8 °C. An average July air temperature is $+18.5$ °C. Mean annual precipitation is 730 ± 56 mm (data averaged from 2013 to 2021 according to the website rp5.ru).

After land abandonment, due to the stopping of agricultural activity, pine reforestation began without any human management, and a space-for-time substitution approach was used to study the changes in soil microbiome. The chronosequence of phytocenoses included agricultural fields, fallow meadows and pine forests. During fieldwork, stages of pine forest sandy soil regeneration from ploughing were identified and sampled in triplication at the key sites located on interflaves, with no signs of excessive waterlogging (Table 1, Fig. S1). The key sites were selected based on the analysis of historical maps and remote sensing

Table 1

Sandy soils and vegetation of pine reforestation stages studied in the Smolenskoye Poozerye national park.

Stage	Soils: soil horizons named according to (IUSS Working Group WRB, 2022)	Vegetation	Distance, km
0	Arenosols (Aric): Ap ₂₆ – C	Agrocenoses and 1–2-year fallows	0.1
1	Entic Rustic Podzols (Ochric) and Arenosols (Ochric): O ₂ – Ap ₂₈ – Bs ₃₇ – C	Meadow fallows 10–25 years on the abandoned agricultural lands	3.4
2	Entic Rustic Podzols (Ochric) and Arenosols (Ochric): O ₃ – Ap ₃₀ – (Bs ₆₀) – C	Young (10–30 years) pine forests on the abandoned agricultural lands	3.6
4	Entic Rustic Podzols (Ochric): O ₃ – A(p) ₂₁ – Bs ₃₉ – C	Medium-aged (60–80 years) pine forests on the abandoned agricultural lands	0.1
5	Entic Rustic Podzols (Ochric) and Arenosols (Ochric): O ₃ – A(p) ₁₇ – (E ₂₃) – Bs ₇₄ – C	Old-aged (80–120 years) pine forests on the abandoned agricultural lands	10.6
6	Rustic Albic Podzols and Entic Podzols (Nechic): O ₄ – A(p) ₆ – (E ₁₁) – Bs ₃₉ – C	Old-aged (90–120 years) "native" pine forests at the non-plough lands or on soils reclaimed after ploughing	16.8

Note. Ecosystems of Stage 3 are not described in this study because the maximum in ploughing area was observed in the study region during the corresponding period. And agricultural land abandoning was not typical for that period. Appropriate pine forests of this age were not found. Initially, we assumed the stage 6 to correspond native forest soils and to be selected as territories consistently forested on the historical materials and remote sensing data (Landsat 1985–2020; Corona 1970). However, during field works, features of former ploughing of the soils, e.g. higher thickness of the humus horizon and higher organic matter content, were found. For only one of the three key sites for a stage 6, we can state with certainty that it has never been used for agriculture. Depth of the lower boundary is indicated for soil horizons. Lowercase figures after horizons, mean depth in cm. Average distance between key sites is represented.

data (from 1927 to 2021) as described in detail in (Shopina et al., 2023; Terekhova et al., 2023). At every key site, two geobotanical descriptions were carried out in plots of 10×10 m for the non-forest stages and 20×20 m for the forest stages. Latin names of the plant species were given according to (Ignatov et al., 2006; Maevskii, 2014). The age of 3–5 trees was determined by trunk cores, taken with an age borer. The period of forest succession was evaluated based on the age of the trees.

Stage 0 includes agrocenoses and young fallows up to 2 years old with domination of grasses and the proportion of short-lived plants reaching 24 % (Table S1). In agrocenoses, the low species diversity (17 species per 100 m²) is associated with the artificial removal of non-target plants. In young fallows, species diversity reaches 40 species per 100 m². Vegetation of stage 1 is represented by old (10–25 years) fallows with short-grass meadow communities with a projective coverage of about 60 % and medium species richness (<30 species per 100 m²). The herb layer was dominated by loose- and long-rhizome *Festuca rubra* and *Poa angustifolia*, as well as the species of genera *Artemisia* and *Potentilla*. Tree species (*Betula* sp., *Pinus sylvestris* and *Populus tremula*) were found only at one key plot and covered <3 %. At stage 2, stands of 10–25 years are formed by pine with an admixture of birches. Approximately 10 years since field abandonment, the tree stand canopy closure results in the herb layer cover decreasing from 80 to 85 % (site 3, Table S1) to 1–20 % (site 1). Meadow species disappear and the participation of forest species increases. Moss cover increases from 5 to 20–45 %. The canopy cover of postagrogenic pine forests of 60–80 years old (stage 4) is 50–70 % with a small admixture of birch. In the undergrowth (projective cover 10–35 %), *Picea abies*, *Quercus robur*, *Sorbus aucuparia*, *Frangula alnus*, *Betula* sp. are present. *Vaccinium myrtillus* dominates the herb layer as its projective cover ranges around 30–70 %.

Mosses cover is 80–100 %. In the postagrogenic pine forests of 80–120 years old (stage 5) the canopy cover is 35–75 % with a small admixture of birch and spruce. At this stage, the pine tree began to die off forming a gap structure. The projective cover of the moss layer varies from 3 to 5 to 50–75 %. At stage 6, the uneven-aged (up to 180 years old) tree stand of the pine with a small admixture of birch has minimal canopy cover (30–45 %). In the herb layer, with a projective cover of 35–80 %, *Vaccinium vitis-idaea* and *V. myrtillus* dominate. Projective cover of the moss layer is 80–100 %.

2.2. Soil sampling, chemical analysis and DNA sequencing

At each key site, soil samples (98 samples of 300–500 g) for the subsequent physical and chemical analysis were taken from cross-sections. The samples of each soil horizon were collected from a perimeter (approximately 3 m) of soil cross-section including the front and side walls of the cross-section. Physical and chemical analyses were conducted using routine standardized techniques (Pansu and Gautheyrou, 2006; van Reeuwijk, 2002) as reported in Table S2 for pH value, soil organic matter content (SOM), available phosphorus (P_{av}), available potassium (K_{av}), total nitrogen (N_{tot}), total carbon (C_{tot}) and granulometric composition. To compare the data sets (i. the upper vs lower layers of the same chronosequence stage; ii. same layers of the different stages) for soil properties, the Mann-Whitney *U* test (p_M) was used. Only significant differences ($p_M < 0.05$) are presented in the Result section.

54 soil samples (6 stages × 3 sites × 3 depths) for the subsequent extraction of total DNA were collected from three groups of vertical locations of each soil cross-section using knifepoint into 1.5 mL tubes. To avoid cross-sample contamination, the first sample was collected from the lower vertical location followed by the middle and upper locations. Prior to sampling, the cross-section sides were cleaned if necessary. The knife was treated with 96 % ethanol before collecting each sample.

The first group of samples (A) was picked from the uppermost part of the A-horizon rich in humus from a depth of 0–0.5 cm directly under the leaf litter (Table S3). According to the pine reforestation stage, three subgroups of the A-horizon were sampled: i. natural (non-modified by ploughing) A-horizon typical for Entic Podzols (Nechic) of Stage 6; ii. Ap-horizon developed due to ploughing with a (very) abrupt distinctness and a smooth shape of the lower boundary according to (IUSS Working Group WRB, 2022) and typical for soils of Stages 0–2; iii. A(p)-horizon preserving signs of modification by ploughing with a gradual distinctness and a wavy shape of the lower boundary according to (IUSS Working Group WRB, 2022) and typical for soils of Stages 4–6. The second group of samples (B) was collected from the lowermost (12–40 cm) part of the A-horizon. The third group of samples (C) was obtained from the uppermost part of the parent material i.e., C-horizon (25–74 cm). The sampling depths of B and C varied depending on the depths of ploughing and the presence of middle horizons (i.e., E-horizon, Bs-horizon; see Table 1) between the ploughing horizon and parent material (Table S3). All samples were taken in at least 5 representative locations from the front and side walls of the cross-section (the total area of sampling is approximately 1 m²), avoiding excavation, charcoals and other disturbances that would affect the composition of the soil microbiota. The soils and soil horizons were classified according to (IUSS Working Group WRB, 2022).

Sample tubes were placed in a – 20 °C freezer at the end of each sampling day and were stored until the end of the fieldwork, and transported to the lab in a frozen state in a food thermos. Total DNA from soil samples was isolated using DNeasy PowerSoil (Qiagen, Germany). Subsamples of 300 mg were put into a PowerBead tube, then 60 µl of the C1 buffer was added, and the tube was inverted 4–5 times to mix the reagents. The samples were then disrupted using TissueLyser II or TissueLyser LT (Qiagen, Germany, 10 min, 30 Hz). Then DNA was purified according to the manufacturer's protocol. Its concentration ranged from 2 to 3 ng/µl on average and was measured on the Qubit 1 fluorimeter

using the Qubit DNA HS kit (Thermo Fisher Scientific, USA).

Variable 16S rRNA regions were amplified with two primer combinations, V3-V4 and V4-V5 (341F 5'–CCTAYGGGRBGCASCAG–3' and 806R 5'–GGACTACNNGGTATCTAAT–3'; 515F 5'–GTGCCAGCMGC CGCGGTAA–3' and 907R 5'–CCGTCAAATTCCTTTGAGTTT–3', respectively). Phusion polymerase (New England Biolabs, USA) and the following program was used for amplification:

Step 1: 95 °C 2 min (initial DNA melting)

24 cycles as follows:

Step 2: 95 °C 30 s (melting)

Step 3: 58 °C 30 s (primer annealing)

Step 4: 72 °C 40 s (synthesis)

Step 5: 72 °C 5 min

The product specificity was checked using electrophoresis in 2 % agarose (1 × Tris-acetate-EDTA buffer, 100 V/14 mA). Gels were visualized on a transilluminator under the UV light. To prepare sequencing libraries, amplicons were purified using the AMPure XP beads (Beckman Coulter, USA) according to the manufacturer's protocol (90 % V:V). Amplicon concentrations were measured on the Qubit 1 fluorimeter using the Qubit DNA HS kit (Thermo Fisher Scientific, USA). Samples (distilled water) containing no DNA processed in the same laboratory were used as a negative control. To skip the adaptor ligation step, all primers already contained Illumina 1 (forward primer) or Illumina 2 (reverse primer) adaptors. Index PCR was made using Phusion polymerase (New England Biolabs, USA) and the Nextera XT Index kit (Illumina, USA) according to the manufacturer's protocols. The library concentrations were measured on the Qubit 1 fluorimeter using the Qubit DNA HS kit (Thermo Fisher Scientific, USA). The libraries were sequenced on Illumina MiSeq with read length of 250 bp (MiSeq Reagent Kit v2).

2.3. Bioinformatics and statistical analyses

The bacterial and archaeal 16S rRNA sequences generated were processed using QIIME 2 version 2022.2 (Bolyen et al., 2019). Demultiplexing the sequence was followed by quality control using DADA2 (Callahan et al., 2016). Taxonomy was assigned to amplicon sequence variants (ASVs) with 99 % similarity using the 16S rRNA SILVA database version 138 (G. Kim et al., 2019). The pre-trained classifier obtained with the RESCRIPt plugin (Robeson et al., 2021), was used. Taxonomic matrices generated were used for further statistical analyses. To assess alpha and beta diversity, a phylogenetic tree was constructed using the fasttree method with MAFFT alignment (Katoh and Standley, 2013; Price et al., 2010).

Two sets of mentioned primers for the two 16S rRNA gene regions were used to confirm the homogeneity of the results (Abellan-Schneyder et al., 2021). The relative abundance of the reads was determined as a proportion of the total reads to account for PCR bias in each different sample. Results for the two variable regions at the family level were highly correlated ($R^2 > 0.66$). However, the V4-V5 region provided more families (460) compared to the V3-V4 region (420), including 109 families not found for the V3-V4 region at all (Fig. S2). Of these 109 families, 5 families had an abundance >50 reads (Micrococcaceae, Streptomycetaceae, Oxalobacteraceae, Burkholderiales A21b, Burkholderiales SC-I-84). For simplicity, results in the main text were obtained from the data on the V4-V5 region, while the plots for V3-V4 regions were provided in the Supplementary Material. This did not influence the conclusions.

Further statistical analysis and data visualization were performed in R 4.1.3 using phyloseq (McMurdie and Holmes, 2013), vegan (Dixon, 2003), caret (Kuhn et al., 2023) and ggplot2 (Kassambara, 2020) packages. Indicator families were identified using the indicpecies package (De Cáceres and Legendre, 2009). Singleton operational taxonomic units (OTUs) were excluded from the analysis, and communities were rarefied to 21,517 sequences per sample.

Permutational Multivariate Analysis of Variance (PERMANOVA),

PPER) from the pairwiseAdonis function from package ‘vegan’ was used to estimate the significance of microbiome differences between the groups of sampling depths (A, B and C) and stages (0–6) using distance matrices obtained with QIIME2 at the ASV level. The Benjamini–Hochberg false discovery rate (FDR) correction for multiple testing was applied. FDR corrected Wilcoxon rank test (p_W) and median effect-size from Aldex2 were used to search for bacterial groups whose proportion differed significantly between the studied conditions (Fernandes et al., 2014; Gloor et al., 2016). The distance matrices obtained in QIIME2 were used for cluster analysis, principal coordinate analysis (PCoA) and t-distributed stochastic neighbourhood embedding (t-SNE) (Xu et al., 2021).

The metabolic potential of the microbial communities was predicted using a PICRUSt2 package for QIIME2 (Douglas et al., 2020). Although the authors understand that there are some limitations and uncertainties in gene assessment using PICRUSt, this approach was shown to be valuable and is frequently used in modern research (Agrawal et al., 2019; Lu et al., 2023; Shang et al., 2023). Differences in metabolic pathway frequencies were assessed with the same statistical tests as described for microbial abundances. The metabolic pathway composition of samples was visualized with Principal Coordinate Analysis (PCoA) of Bray-Curtis distances.

Similarities in the physical and chemical properties of the studied soils were shown using Principal Component analysis (PCA). To assess

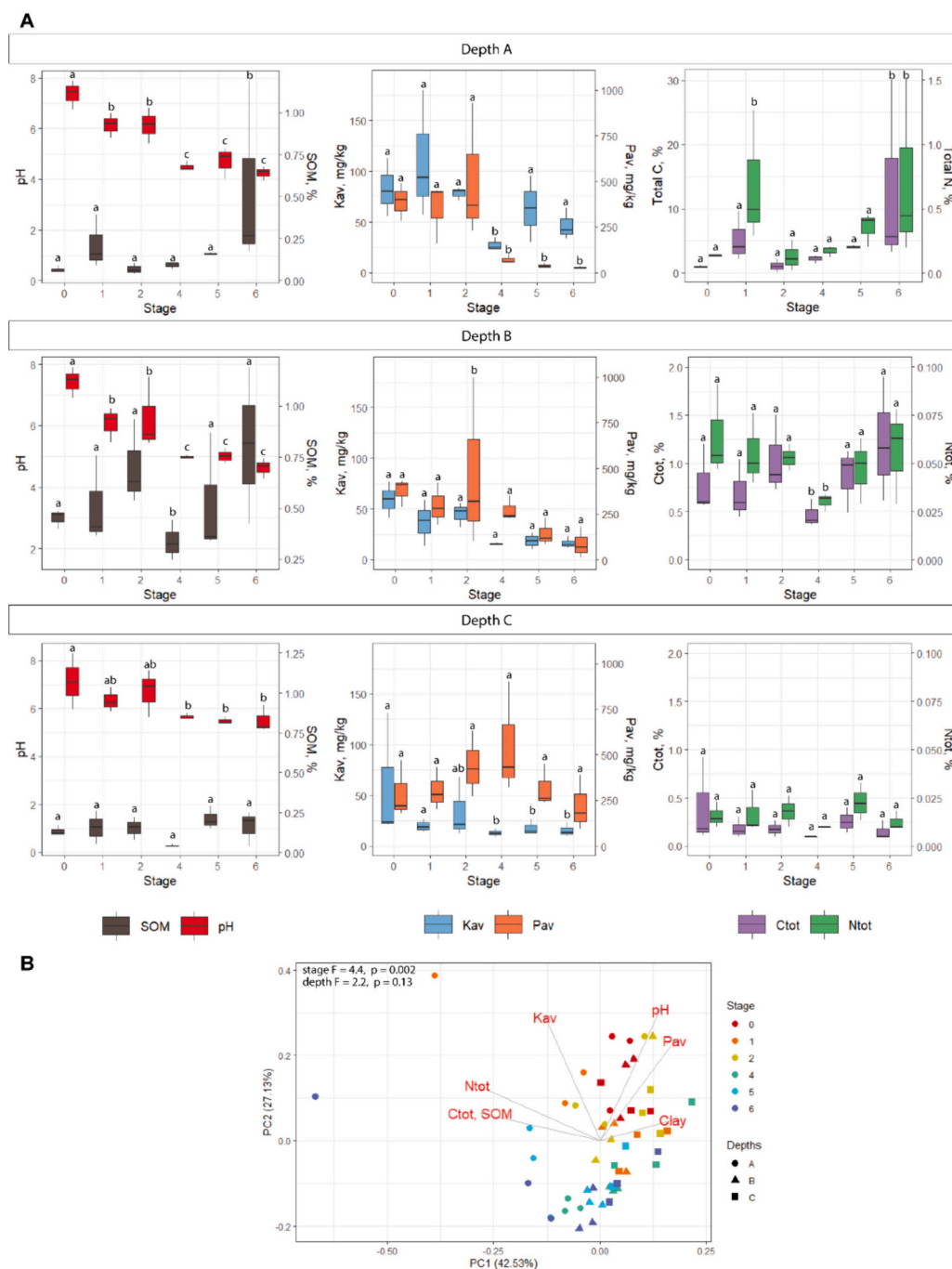


Fig. 1. Differentiation of studied soils of stages 0–6 of the chronosequence in the Smolenskoye Poozerye National Park. A – soil properties by stages. Upper case letters A, B and C correspond to sampling depths. Lower case letters a, b and c indicate significant differences between stages for each parameter at $p = 0.05$. B – PCA of the soil chemical properties. PERMANOVA F-ratios and ps are provided for stage and depth used as predictors.

the impact of physical and chemical soil properties on the structure of the microbiome and its predicted metabolic pathways, a random forest model was used as follows. The clustering results by Ward's minimum variance method with the weighed UNIFRAC distances for microbiome composition and Bray-Curtis distances for predicted metabolic pathways composition were used to classify samples with similar microbiome and metabolic pathway structure. The optimal number of clusters was chosen to be 3, as a larger number of clusters would result in single-sample clusters, which would degrade the quality of the model. The results of clustering were used in a random forest model where physical and chemical soil parameters as well as sampling horizons and stages were used as predictors. The resulting models had 100 and 90 % accuracy for microbiome and predicted metabolic pathways composition, respectively. The variable importance scaled scores were used to evaluate the impact of soil properties on microbiome composition (Breiman, 2001). Because non-parametric statistical tests were used, tests for normality and homogeneity were not carried out for the data since multivariate compositional data usually does not meet the criteria for multivariate normality.

3. Results

Most of the horizons of the studied soils were (loamy) sand or sandy loam. Singular samples of the B-horizon and parent materials were classified as (silty) loam or silt. It confirms the similarity of parent materials of all soils studied and the formed chronosequence does not differ in texture. The pH level of the studied soils ranged from acidic to slightly alkaline. In most soils, the pH values did not change or increased slightly with a depth (from A to C depths, Fig. 1). The maximum pH values were typical for ploughing soils at stage 0 ($p_M < 0.05$ with all other stages). Further on, by stage 6, the pH values fell monotonically.

Content SOM, Kav, Pav, Ctot and Ntot decreased with depth in all soils. In the A horizon, SOM content rose through chronosequence reaching a maximum at stage 6. At the lowermost part of A-horizon and the uppermost part of C-horizon, minimum SOM content was at stage 4. At the uppermost part of A-horizon, Pav content decreased through chronosequence. At the same time, the content of Ctot and Ntot had a local maximum at stage 1 and linearly increased from stage 2 to 6. Kav content showed a minimum at stage 4 at all depths. This sharp fall in its content from stage 2 to stage 4 was also true for Ctot and Ntot at the lowermost part of A-horizon and the uppermost part of C-horizon. At the uppermost part of C-horizon, Pav content rose from stage 0 to stage 4 and then decreased.

Variations in the studied soil properties differed highly between samples of stages for the uppermost and lowermost part of the A-horizon. Samples of the uppermost part of the C-horizon were more consistent (Fig. 1).

3.1. The taxonomic composition of a soil microbiome

Proteobacteria (13–36 %), Actinobacteriota (8–33 %), Acidobacteriota (8–29 %), Planctomycetota (1–20 %) and Chloroflexi (0.03–16 %) dominated in all soil microbial communities considered. In general, the set of the 10 most common phylum varied slightly with depth (Fig. S4).

3.1.1. Vertical differentiation

The uppermost and lowermost part of the A-horizon had an identical compositional set, whereas, for the C-horizon, the top 10 phyla included Verrucomicrobiota (0.1–4 %) and Methyloirabilota (0.2–4 %) instead of RCP2–54 (0.05–11 %) and Bacteroidota (0.3–6 %). At the ASV level, the microbial composition of the uppermost and lowermost part of A-horizon was similar ($p_{PER} = 0.061$) and differed with C-horizon ($p_{PER} = 0.001$ and 0.002 , respectively). The uppermost and lowermost parts of the A-horizon had no phyla with significant differences. The abundance of Planctomycetota (A depth: 13 % > C depth 6 %, $p_W < 0.0005$),

Bdellovibrionota (A depth: 0.5 % > C depth 0.3 %, $p_W < 0.0005$) and Bacteroidota (A depth: 3 % > C depth 1.2 %, $p_W < 0.0005$), Methyloirabilota (A depth: 0.2 % < C depth 2 %, $p_W < 0.0005$) differed significantly between the uppermost parts of the A and C horizons (effect size >1). Bacteroidota also had a higher abundance at the B depth compared to the C depth (B depth: 2.8 % > C depth 1.2 %, $p_W = 0.0008$). Significant differences in abundance (effect size >1) were observed for the several bacterial families (Fig. S4, Table S4).

Kallotenuales AKIW781 and Hymenobacteraceae were indicator families for the uppermost part of the A-horizon. For the C-horizon, 18 families were indicators (Table S5). No indicator families were found for the lowermost part of the A-horizon.

3.1.2. Temporal differentiation

At the ASV level, soil microbiome composition differed significantly in stages 0–2 compared to stages 4–6 ($p_{PER} < 0.01$). Also, the soil microbiome composition of stage 0 differed significantly with all stages ($p_{PER} < 0.01$). There were no significant differences between stages 1 and 2 ($p_{PER} = 0.16$) and between stages 4, 5, and 6 ($p_{PER} > 0.18$).

As the group for one depth and one stage consisted of 3 samples each, no significant differences were found between stages within the horizon. Therefore, for further analysis of microbiome composition, 2 groups of stages were identified: early stages (0,1,2) and older stages (4, 5, 6). The stages were grouped this way for several reasons. Firstly, as can be seen on the PCA graph (Fig. 1), soil from groups 0, 1, 2 and 4, 5, 6 formed two separate clusters, when it comes to the uppermost and lowermost part of the A-horizon. So that these two groups had more similarities in soil properties, too. Secondly, the same two groups can be identified by analyzing α -diversity. Early-stage soils (especially at A depth) were characterized by higher α -diversity with Shannon index 8–9 (Fig. S5). At the B depth, it decreased more monotonically with the chronosequence stage. At the uppermost part of the C-horizon, the α -diversity was lower in general and the differences between stages became less noticeable. Finally, to confirm the similarity of the composition of the soil microbiome from the early and older stages, a cluster analysis was carried out. Stages 0, 1 and 2 formed a separate cluster for the two parts of the A-horizon. For the uppermost part of the C-horizon, this cluster became less obvious as the composition of the soil microbiome of the different stages became more homogeneous than in the A and B depths (Fig. S6).

In general, samples from the two parts of the A-horizon were grouped by a succession stage (Fig. S3). Early-stage soils and soils of older forests occupied different parts of the plot. Distances between samples of the same stage were relatively short for stage 0 and stage 4 which is in agreement with the close location of the sampling sites corresponding to these two stages (see Table 1). In Fig. 2, the longest distances within a stage were typical for stages 1, 2 and 5. Samples from stage 6 showed higher heterogeneity at depth B than at depth A. Samples from the uppermost part of the C-horizon did not show significant clustering according to a succession stage. On the PCoA space, they were predominantly grouped in the upper left corner.

The weighted UNIFRAC distance was then used as input to t-SNE for unsupervised dimensional reduction (to two dimensions) and visualization (Fig. 2). Predominantly, samples from all depths of stages 0, 1 and 2 clustered together, while samples from these three depths of stages 4, 6 and partly 5 formed three distinct clusters.

Among the 20 most abundant phyla, four groups were identified according to their abundance change during reforestation (Fig. S7). The abundance of 102 and 75 families differed significantly ($p_W < 0.05$, effect size >1) at the uppermost and lowermost part of the A-horizon, respectively (Fig. 3, Fig. S9). At the uppermost part of the C-horizon of older stages, abundance of Anaeromyxobacteraceae, Gammaproteobacteria WD260, Babeliaceae and Obscuribacteraceae was higher ($p_W < 0.05$, effect size >1).

The soil microbial community had 21 indicator families at stage 0 (Table S6). For stages 1 and 2, only two (Phycisphaerae mle1–8 and Gaiellaceae) and one (Cryptosporangiaceae) families were indicators,

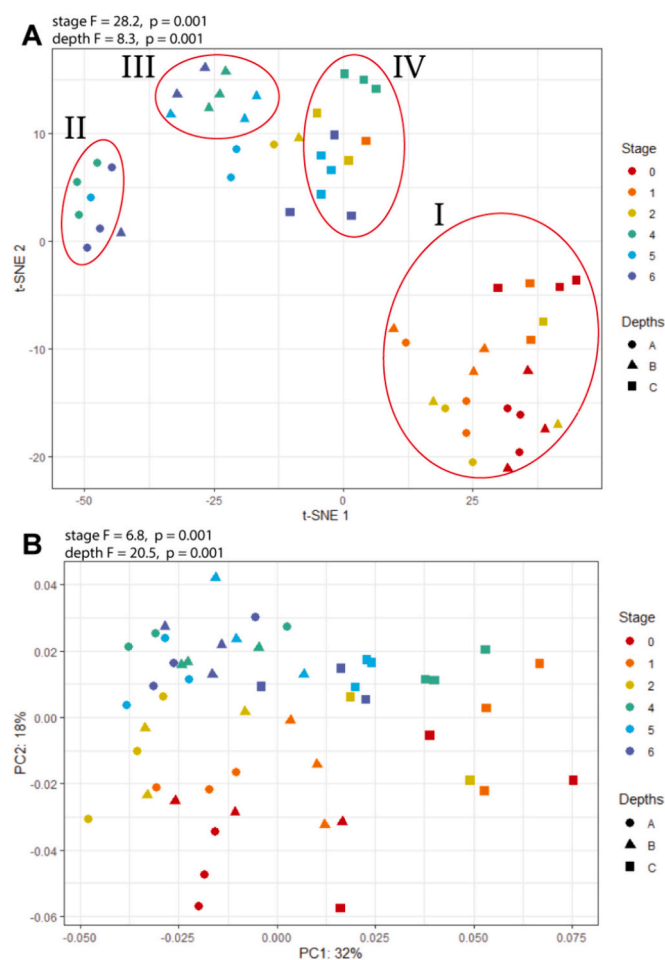


Fig. 2. Differentiation of the soil microbiome composition of stages 0–6 sampled at depths A, B and C. A – the t-SNE plot with a weighted UNIFRAC distance for the V4–V5 region. Clusters (highlighted manually): I – soils of early stages (0, 1, 2); II – A depth of older stage soils (4, 5, 6); III – B depth of older stage soils; IV – C depth of older stage soils; B – PCoA plot based on the relative abundance of predicted metabolic pathways of the soil microbiota with a Bray-Curtis distance for the V4–V5 region. PERMANOVA F-ratios and ps are provided for stage and depth used as predictors.

respectively. There were no indicator families found for the soils of stage 4. Sporolactobacillaceae and Pectobacteriaceae were indicator families for stages 5 and 6, respectively. Early stages (0, 1 and 2) had 60 indicator families, while only Puniceococcaceae and Simkaniaceae were indicators for older stages (4, 5 and 6).

Assessing the contribution of all factors to the microbiome composition by a random forest model showed that the most important soil property was pH with a score of 100, followed by the stage of post-agricultural succession (score 40). Other parameters with high scores were Ctot, Ntot and Pav (29, 17 and 15, respectively; Table S8).

3.2. Metabolic pathways

The most common predicted metabolic pathways in the soils studied were biosynthesis of amino-acids, cofactors, nucleotides, lipids, and carbohydrates responsible for about 70 % of all pathways found.

3.2.1. Vertical differentiation

The metabolic pathway structure of the microbial communities differed significantly at depths A and C ($p_{PER} = 0.024$) and was similar in the pair of depths A and B, and B and C ($p_{PER} = 0.081$ and 0.226, respectively). The abundance of 26 individual pathways differed

significantly in the soil microbiome sampled at the uppermost parts of the A and C horizons ($p_W < 0.05$, effect size >1). Mono-trans, poly-cis decaprenyl phosphate biosynthesis was significantly more abundant at depth A (0.06 %) compared to depth B (0.04 %). Hexitol fermentation to lactate, formate, ethanol and acetate was significantly more frequent at depth C (0.05 %) compared to depth B (0.03 %).

3.2.2. Temporal differentiation

From PERMANOVA results, metabolic pathway abundance and structure were significantly different for stages 1 and 4, 1 and 5, 1 and 6 ($p_{PER} = 0.001$ for three pairs), 2 and 5 (0.041), 2 and 6 (0.15). In the PCoA space with a Bray-Curtis distance, no separation was observed for the samples from the different parts of the A-horizon (Fig. 2). Their position depended predominantly on the stage of succession and not on the horizon: from top to bottom of the plot, samples from the older stages (4, 5, 6), the early stages (0, 1, 2) and from the C-horizon (all stages) formed separate clusters.

Since the frequency of a large number of predicted metabolic pathways – 296 and 260 for the uppermost and lowermost part of the A-horizon, respectively – differed significantly ($p_W < 0.05$, effect size >1) between chronosequence stage groups, further analysis was conducted with a high and low-level grouping of predicted metabolic pathways (7 and 58 groups in total, respectively). At the high level, the abundance of microbial activation-inactivation-interconversion, biosynthesis, degradation, energy metabolism, metabolic clusters and superpathways differed between early and older stage soils (Fig. S10). However, only the activation-inactivation-interconversion group decreased during reforestation ($p_W < 0.05$, effect size >1).

Among 58 predicted metabolic pathways groups examined for all A-horizon samples of early and older stages, 42 groups differed significantly ($p_W < 0.05$, effect size >1 ; Fig. 3). Of these, alcohol-degradation, amino-acid-degradation, interconversion, methylaspartate cycle, phospholipases, superpathway of chorismate metabolism were more abundant at the early stages. For the older stages, 36 groups dominated (most abundant were biosynthesis of amino acids, nucleotides, lipids, carbohydrates, and cell structure).

For the lowermost part of the A-horizon, 13 groups of predicted metabolic pathways differed ($p_W < 0.05$, effect size >1 , Fig. S12). Of these, 8 groups of predicted metabolic pathways dominated at the older stages [degradation of steroids (early stages 0.01 < 0.05 % older stages) and polymers (0.44 < 0.54 %), other degradation (0.09 < 0.2 %), a sulphate assimilation and cysteine biosynthesis superpathway (0.5 < 0.6 %), isopropanol biosynthesis (engineering, 0.11 < 0.16 %), aldehyde degradation (0.0005 < 0.002 % older stages), photosynthesis (0.22 < 0.27 %), a D-glucarate and D-galactarate degradation superpathway (0.05 % < 0.06 %)]. And only 5 groups of predicted metabolic pathways dominated at the early stages [amino acid degradation (early stages 0.95 > 0.65 % older stages), interconversion (0.1 > 0.03 %), chorismate metabolic superpathway (0.2 > 0.1 %), methylaspartate cycle (0.04 > 0.005 %), biosynthesis of siderophores (0.09 > 0.06 %)]. The abundance of predicted metabolic pathways was similar in the C-horizon of the different stages.

The relative importance of soil properties for predicted metabolic pathways composition decreased from pH (score 100) to SOM (51), soil horizon (30), Pav (28) and Kav (12).

4. Discussion

4.1. The taxonomic composition of a soil microbiome

Predominant soil phyla observed in our studies belonged to the groups of the most abundant bacteria phyla worldwide (Delgado-Baquerizo et al., 2018) and the core microbiome group of the East-European plain (Pershina et al., 2018; Semenov et al., 2023; Shelyakin et al., 2022). It was similar to microbiomes of other forest (Cao et al., 2021; Chen et al., 2021; Pressler et al., 2020; Shao et al., 2019; Shelyakin

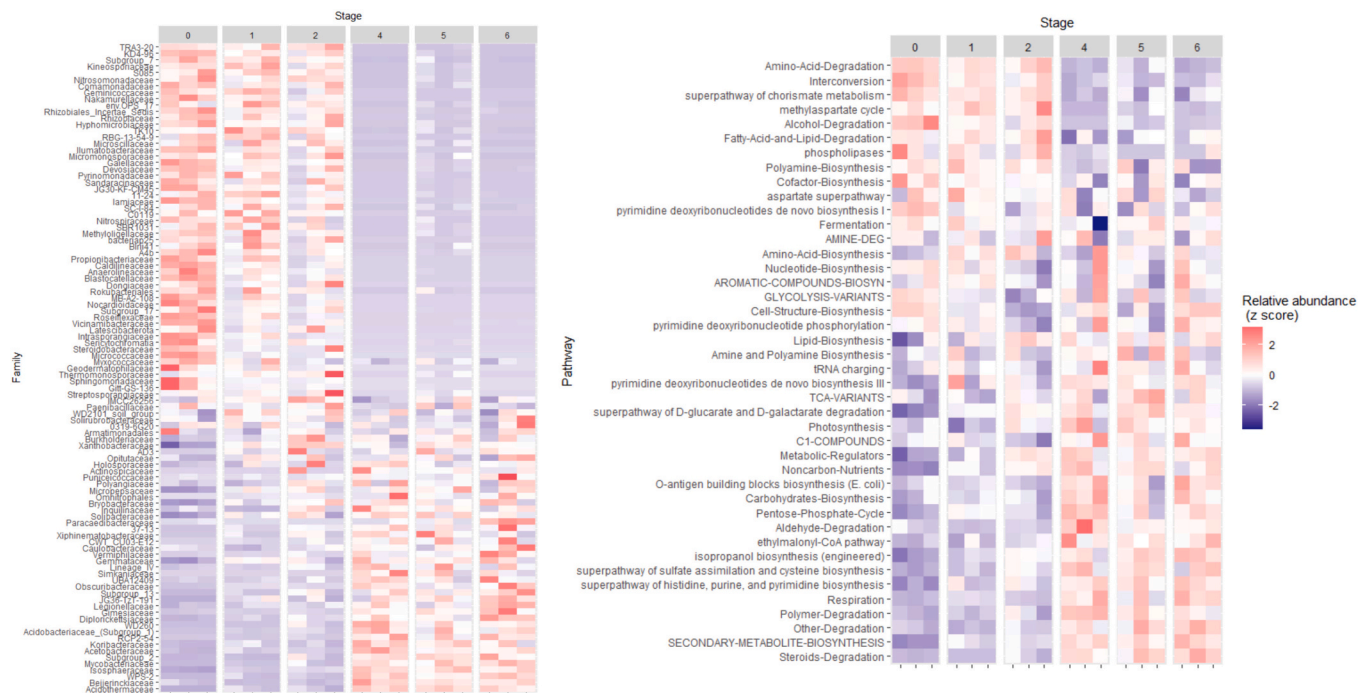


Fig. 3. Heatmap with relative abundance of bacterial families (left) and lower-level grouping metabolic pathways groups (right) differed significantly ($p_W < 0.05$) between early and older succession stages at the uppermost and lowermost part of the A-horizon for the V4-V5 region. The abundance of each bacteria family is scaled (z-score) across all samples.

et al., 2022; Bereczki et al., 2024; Zhou et al., 2023) and ploughing soils (Górska et al., 2024), as well as soils of abandoned croplands (Abakumov et al., 2023; Gao et al., 2023; Liu et al., 2024).

4.1.1. Vertical differentiation

Our results showed that the microbial community of the uppermost and lowermost part of the A-horizon does not differ even in soils of older stages of the post-agrogenic succession. This could mean that for >15 cm of the (previously) ploughing horizon, soil metagenome stays uniform, since the lower boundary of the A(p) horizons is laid on the depth of 15–27 cm in the studied soils. Differences in the microbial community between the uppermost and lowermost part of the A-horizon became evident at the older chronosequence stages (4, 5, 6) based on the results of the t-SNE analysis. The homogeneous composition of the Ap horizon microbiome resulted from mixing during ploughing preserved for 30 years. While at the older stages, soil-forming processes e.g., eluviation and/or podzolization lead to the differentiation of the previously ploughed horizon. Higher heterogeneity of microbiomes of older Podzols at the East-European plain was shown previously (Ivanova et al., 2020). The microbiome of the C-horizon always differed significantly from the microbiome of the topsoils due to the vertical differentiation of the chemical and physical soil properties (Tripathi et al., 2019). In arable lands, the taxonomic composition of the soil bacterial community is differentiated according to the depth of tillage and associated fertilizing (Kim et al., 2021; Zhong et al., 2023).

Our results on the differentiation of abundance of bacterial taxa are in agreement with the previous studies (Table S4) e.g., for highly frequent in the studied topsoil Bacteroidota, Planctomycetota and Planctomycetota. Despite the total number of families being lower in soil-forming material samples, more indicator families were found for the C-horizon compared to the A-horizon. The microbiome of the C-horizon had lower α -diversity than reported previously (Islam et al., 2022; Shao et al., 2019) and more unique taxa which probably could not inhabit topsoil horizons due to the environmental gradient described above.

4.1.2. Temporal differentiation

Our results showed that the microbiome composition of ploughing soils contrasted with soils of all other pine reforestation chronosequence stages. Ploughing soils had maximum α -diversity and number of indicator families. These soils had a minimum relative abundance of Planctomycetota and a maximum abundance of Cyanobacteria from all the stages. The diversity of microorganisms increased probably due to fertilization and aeration improving ecological conditions for microorganisms. Inorganic nitrogen fertilizer and compost altered the diversity and structure of the soil bacterial community in the case of cultivation of buckwheat (*Fagopyrum esculentum* Moench) (Morigasaki et al., 2024).

Higher α -diversity and number of indicator families in the topsoil were typical for all early-stage soils. Only two indicator families with higher abundance were characteristic for older stages. So, α -diversity dropped significantly after 70 years of reforestation due to depletion as sandy soils themselves are poor in nutrients. Previously, in abandoned croplands situated on Podzols, the highest α -diversity was reported for 40-year-old soil which decreased with the increasing time of the fallow state (Lavrishchev et al., 2024). Higher bacterial diversity in ploughed soils in comparison with forest soils was also reported in the Amazon region (Pressler et al., 2020) and in China (Chen et al., 2021; Wang et al., 2022; Yang et al., 2022). Post-logging succession in China also showed a decrease in microbial diversity in plantations (Islam et al., 2022). Microbial diversity decreases with the age of land abandonment in the southern taiga of Russia (Ivanova et al., 2020) and with a stand age in China (Shao et al., 2019). Although some studies show no significant differences in diversity during reforestation (Chernov et al., 2021; Gao et al., 2023) or increase in diversity with succession (Cao et al., 2021). Also, the microbiome composition of soils from stage 2, on which the tree layer is already formed, was more similar to meadow soils than to the older forest soils. This indicates that reforestation occurs faster than the recovery of soil microbiome.

No linear trend was observed for β -diversity. The highest spatial homogeneity was characteristic of the soils of stages 0 and 6 for the uppermost part of the A-horizon. Stage 0 was characterized by the most favourable environmental conditions, while stage 6 was the least

favourable. Perhaps at these extremes, spatial heterogeneity starts to play a lesser role. It is interesting to note that *Methylomirabilota* had maximum relative abundance at stages 0 and 6, which may indicate that both ploughed and non-disturbed soils are equally favourable for some groups of bacteria. On the other hand, *Elusimicrobiota* had the lowest abundance at these two stages, which means this phylum prefers moderate anthropogenic disturbance of the soils. Another conclusion to be drawn from the β -diversity analysis and differentially abundant families is that for all parts of the A-horizon, the composition of the soil microbiome is more dependent on the stage of the pine reforestation chronosequence than on the depth. Whereas for parent materials, the stage of the pine reforestation chronosequence plays a minor role. So, changes in the soil metagenome during pine reforestation chronosequence affect about the upper 30 cm layer i.e., the previously ploughed horizon.

Ordination methods in other studies also showed distinct clustering of the soil microbiome composition according to a chronosequence stage (Chen et al., 2021). In younger forests in Vietnam, a soil microbiome structure was more similar to agricultural soils, whereas in older forest plantations, it was more similar to native forests (Chernov et al., 2021). This corresponds greatly with our results. However, in a study from China, while soil samples clustered according to a chronosequence stage, soil depth played an important role in clustering (Islam et al., 2022).

Similar to our results higher abundance of *Acidobacteria* in forest soils compared to agricultural soils was shown in the Amazon region (Pressler et al., 2020), Central Hungary (Bereczki et al., 2024) and New Zealand (Hermans et al., 2020). A higher abundance of *Verrucomicrobiota* and *Dependentia* was observed in primary forests (Qi et al., 2020; Shao et al., 2019) and in pine plantations in Argentina (Trentini et al., 2020), respectively. The abundance of RCP2–54 phylum negatively correlated with Ntot content (Muhammad et al., 2022), which could also decrease in our case with a chronosequence stage due to the depletion of nutrients added with fertilizers. However, a decrease and increase in *Verrucomicrobiota* during reforestation was found in China (Islam et al., 2022) and in Hungary (Bereczki et al., 2024), respectively, while another study stated a decrease in the abundance of *Acidobacteria* (Shao et al., 2019). Some studies showed a higher abundance of *Proteobacteria* in native forests (Hermans et al., 2020; Bereczki et al., 2024; Qi et al., 2020), while in our case their abundance was constant for all stages. Also, in contrast with our results, several studies show a decrease in WSP-2 in forest soils (Qu et al., 2020; Sheremet et al., 2020). On the other hand, over-representation in agricultural soils of *Actinobacteria*, *Chloroflexi*, *Gemmatimonadetes*, *Bacteroidetes*, and *Nitrospira* shown in our study was also observed in the Amazon region (Pressler et al., 2020). However, a studies showed a decrease in *Actinobacteria* (Shao et al., 2019) and an increase in *Bacteroidota* and *Gemmatimonadota* (Bereczki et al., 2024). *Myxococcota* preference for ploughing soils was shown in Switzerland (Gschwend et al., 2022). But in contrast to our results, *Latescibacterota* abundance was shown to increase with reforestation (Lan et al., 2022). For similar chronosequence with Podzols sampled 370 km further to the North, fallow soils were abundant in *Nitrosomonadaceae* (*Pseudomonadota*), *Mycobacterium* (*Actinobacteria*), *Nitrospira* (*Nitrospirota*), and *Luteolibacter* (*Verrucomicrobiota*) (Lavrishchev et al., 2024).

The number of differentially abundant families between stages was close for the uppermost and lowermost part of the A-horizon, while dropped significantly in the C horizons which means that the parent materials were less influenced by ploughing. Thus, approximately the upper 30-cm of soil is altered the most during pine reforestation.

4.2. Metabolic pathways

4.2.1. Vertical differentiation

Although in microbiome composition depths B and C differed significantly which was not inconsistent with a predicted metabolic pathways structure, the abundance of predicted metabolic pathways

differed significantly only for A and C depths. So, the taxonomic structure of the soil microbiome changed more rapidly with depth than the predicted metabolic pathways. There should be some bacterial taxa that substitute each other in terms of predicted metabolic pathways. However, this question required additional research.

Most of the predicted metabolic pathways with higher abundance at the uppermost part of the A-horizon were related to vitamin K and its precursor biosynthesis which are involved in bacterial electron transport and in sensing environmental changes such as alterations in redox state (Gajare et al., 2016; Stavridou et al., 2021) that also changes during pine reforestation. Probably, in the surface horizons, the redox conditions change more often due to varying air access (Enchilik et al., 2023). Under usual conditions, there is good aeration here, but this changes after rain falls. Consequently, the bacteria producing menaquinones are therefore more fit at the uppermost part of the A-horizon (Kang et al., 2022). Other pathways more widely observed in the topsoils included C1 compounds (including methanol) oxidation to CO₂. This could be explained by the higher concentration of such gases in the subsoil. Methane and methanol mostly enter the soil from plant decomposition and exudates. Thus, the soil layer underlain by the litter should be enriched in one-carbon compounds (Kolb, 2009).

The rest of the pathways more abundant at the uppermost part of the A-horizon were from the degradation group. Bacteria from the topsoil were more engaged in aromatic compound degradation probably due to higher concentrations of such substances in the A-horizon. A higher frequency of salicylate degradation at the uppermost part of the A-horizon could also be connected to the degradation of aromatic compounds since it is a common intermediate in the degradation of a lot of them. Moreover, salicylate is additionally produced by plants in soil and hence also has a higher concentration in the topsoil. Finally, the microbiome at the uppermost part of the A-horizon had a higher 1,5-anhydrofructose degradation potential. Fructose is plant-delivered and has higher content in topsoils (Gunina and Kuzyakov, 2015).

At the uppermost part of the C-horizon, on the other hand, there were several more abundant pathways of biosynthesis of organic substances due to its lack here (Zheng et al., 2024). Many of these pathways are Archaea-produced and caused by their higher abundance (Turner et al., 2017). The reason for higher denitrification and sugar alcohols and fucose degradation observed at the uppermost part of the C-horizon was uncertain since the alcohol degradation rate was known to rise with the addition of nutrients and oxygen (Ang and Abdul, 1992), which are limited in the C-horizon. Denitrification activity is also shown to be maximum in the topsoil (Luo et al., 1998). Another main factor altering biosynthesis in the C-horizon is the high pH value (Zhang et al., 2024).

4.2.2. Temporal differentiation

Metabolic pathway composition was also quite contrast between early-stage and older-stage soils. Similar to microbiome composition, it was affected mostly in the topsoil. However, the gap in the number of differentially abundant groups of pathways by stages between the uppermost and lowermost part of the A-horizon was greater than in the number of differentially abundant families. It means that reforestation affects soil to a shallower depth in terms of predicted metabolic pathways.

The most obvious decrease in the number of pathways with the stage of pine reforestation chronosequence was observed for activation-inactivation-interconversion. This shows that while for the whole soil changes in major chemical modifications fluctuate, the activity of minor chemical modifications provided by soil microorganisms drops with reforestation, especially during the first 30 years.

Looking at the pathways of microbial communities at the early stages, higher abundance was typical for the degradation of alcohols and amino acids, which could be explained by higher amounts of nutrients. Amino acid decomposition was also shown to increase with soil temperature and respiration, content of Ctot and Ntot (Jones, 1999; Kemmitt et al., 2008). A methylaspartate cycle was more abundant probably

due to a higher diversity of microorganisms in the early-stage soils, which use alternative substances for assimilation such as acetate (Tang et al., 2011). The same could be true for chorismate metabolism. Higher activity of phospholipases in soils was associated with soil pH (Kuroshima and Hayano, 1982). Also, early stages showed more siderophores biosynthesis, which means the microbial community was more able to uptake metals, especially Fe, which could be explained by the lower available metal concentration in soils of early stages due to higher pH levels (Bakker et al., 2014). A higher capacity for carbon metabolism is typical for (previously) arable soils in comparison with non-cultivated (Liu et al., 2024; Song et al., 2024) and for soil horizons rich in SOM (Zheng et al., 2024).

Older stages showed more pathways with higher abundance. Therefore, while α -diversity decreased with forest age, the number of diverse pathways increased. Differentially abundant predicted metabolic pathways included some degradation ones but mostly was biosynthesis. Rates of fermentation, photosynthesis, non-organic nutrient assimilation and respiration were higher at older stages.

5. Conclusions

Our original hypothesis was partially proven. Pine reforestation significantly altered the sandy soil microbiome composition. The abundance of a number of predicted metabolic pathways increased with restoration, although α -diversity decreased. The 0–30 cm topsoil layer was the most affected by pine reforestation. As sandy ploughing lands could provide more diversity and some phyla behave the same for the initial and final stages of the post-agrogenic chronosequence, pine reforestation at the poor sandy soils may not be beneficial for the soil microbiome.

Our results showed that the importance of soil parameters influencing general microbiome composition and composition of predicted metabolic pathways are different. Although pH was the most important factor in explaining both the set of predicted metabolic pathways and microbial composition of soils. The importance of other parameters varied. The stage of pine reforestation chronosequence influenced microbiome composition greatly. While its impact on predicted metabolic pathways composition was less visible. On the other hand, the content of SOM was more important for predicted metabolic pathways than for microbiome composition.

Pine reforestation of ploughing lands can significantly alter the relative abundance of the dominant soil bacteria as well as the predicted metabolic pathways they possess. In detail, it increases the abundance of Acidobacteriota, RCP2–54, Verrucomicrobiota, Dependenteae, and WPS-2, while decreases the abundance of Actinobacteriota, Chloroflexi, Gemmatimonadota, Myxococcota, Bacteroidota, Latescibacterota, Nitrospirota in soils studied in the Smolenskoye Poozerye National Park. Bacterial biosynthesis, fermentation, photosynthesis and respiration rise with pine reforestation. The upper 30-cm layer of soils is suggested as the best indicator of microbiome disturbance during post-ploughing restoration.

Soil microbiome restoration occurs slower than tree layer restoration. A tree layer is formed in 10–30 years, while soil microbiological composition still has more resemblance to sandy soils under the fallow lands and meadow fallow. The results obtained can be used in the environmental assessment to evaluate the degree and the rate of restoration of soils in impacted areas.

Funding

This work was supported by the RSF project No. 21-74-20171.

CRedit authorship contribution statement

Olga V. Shopina: Writing – original draft, Formal analysis. **Aleksey I. Bondar:** Writing – review & editing, Investigation, Formal analysis.

Elena V. Tikhonova: Writing – review & editing. **Anastasiya V. Titovets:** Writing – review & editing. **Ivan N. Semenov:** Writing – review & editing, Funding acquisition.

Declaration of competing interest

The authors declare that they have no known competing financial interests or personal relationships that could have appeared to influence the work reported in this paper.

Data availability

Data will be made available on request.

Acknowledgments

Content of Kav, Pav, Ntot and Ctot was determined in the laboratory of the Institute of Biology Komi SC UrD RAS. Sequencing service was provided by the Genomics Core Facility of the Skolkovo Institute of Science and Technology. The authors thank Yu.B. Bachinsky, D.R. Bardashov, E.V. Basova, V.R. Khokhryakov, G.V. Klink, D.N. Tikhonov for their assistance in fieldwork, E.A. Gavriluk and I.M. Bavshin for their assistance in preliminary choice of key sites.

Appendix A. Supplementary data

Supplementary data to this article can be found online at <https://doi.org/10.1016/j.apsoil.2024.105570>.

References

- Abakumov, E.V., Gladkov, G.V., Kimeklis, A.K., Andronov, E.E., 2023. The microbiomes of various types of abandoned fallow soils of South Taiga (Novgorod Region, Russian North-West). *Agronomy* 13 (10), 2592. <https://doi.org/10.3390/agronomy13102592>.
- Abellan-Schneyder, I., Machado, M.S., Reitmeier, S., Sommer, A., Sewald, Z., Baumbach, J., List, M., Neuhaus, K., 2021. Primer, pipelines, parameters: issues in 16S rRNA gene sequencing. *mSphere* 6 (1). <https://doi.org/10.1128/msphere.01202-20> e01202–20.
- Agrawal, S., Kinh, C.T., Schwartz, T., Hosomi, M., Terada, A., Lackner, S., 2019. Determining uncertainties in PICRUSt analysis – An easy approach for autotrophic nitrogen removal. *Biochem. Eng. J.* 152, 107328 <https://doi.org/10.1016/j.bej.2019.107328>.
- Ahti, T., Hämet-Ahti, L., Jalas, J., 1968. Vegetation zones and their sections in northwestern Europe. *Ann. Bot. Fenn.* 5 (3), 169–211.
- Ang, C.C., Abdul, A.S., 1992. A laboratory study of the biodegradation of an alcohol ethoxylate surfactant by native soil microbes. *J. Hydrol.* 138 (1–2), 191–209. [https://doi.org/10.1016/0022-1694\(92\)90164-Q](https://doi.org/10.1016/0022-1694(92)90164-Q).
- Bakker, P.A.H.M., Ran, L., Mercado-Blanco, J., 2014. Rhizobacterial salicylate production provokes headaches! *Plant and Soil* 382 (1–2), 1–16. <https://doi.org/10.1007/s11104-014-2102-0>.
- Baldrian, P., López-Mondéjar, R., Kohout, P., 2023. Forest microbiome and global change. In: *Nature Reviews. Microbiology*. <https://doi.org/10.1038/S41579-023-00876-4>.
- Berezki, K., Tóth, E.G., Szili-Kovács, T., Megyes, M., Korponai, K., Lados, B.B., Illés, G., Benke, A., Márialigeti, K., 2024. Soil Parameters and Forest Structure Commonly Form the Microbiome Composition and Activity of Topsoil Layers in Planted Forests. *Microorganisms* 12, 1162. <https://doi.org/10.3390/microorganisms12061162>.
- Bolyen, E., Rideout, J.R., Dillon, M.R., Bokulich, N.A., Abnet, C.C., Al-Ghalith, G.A., Alexander, H., Alm, E.J., Arumugam, M., Asnicar, F., Bai, Y., Bisanz, J.E., Bittinger, K., Brejnrod, A., Brislawn, C.J., Brown, C.T., Callahan, B.J., Caraballo-Rodríguez, A.M., Chase, J., Caporaso, J.G., 2019. Reproducible, interactive, scalable and extensible microbiome data science using QIIME 2. In: *Nature Biotechnology*, Vol. 37, Issue 8. Nature Publishing Group, pp. 852–857. <https://doi.org/10.1038/s41587-019-0209-9>.
- Breiman, L., 2001. Random forests. *Mach. Learn.* 5 (32), 5–32. <https://doi.org/10.1023/A:1010933404324>.
- Callahan, B.J., McMurdie, P.J., Rosen, M.J., Han, A.W., Johnson, A.J.A., Holmes, S.P., 2016. DADA2: high-resolution sample inference from Illumina amplicon data. *Nat. Methods* 13 (7), 581–583. <https://doi.org/10.1038/nmeth.3869>.
- Cao, H., Du, Y., Gao, G., Rao, L., Ding, G., Zhang, Y., 2021. Afforestation with *Pinus sylvestris* var. *Mongolica* remodelled soil bacterial community and potential metabolic function in the Horqin Desert. *Global Ecology and Conservation* 29, e01716. <https://doi.org/10.1016/j.gecco.2021.e01716>.
- Chen, M., Zhu, X., Zhao, C., Yu, P., Abulaizi, M., Jia, H., 2021. Rapid microbial community evolution in initial *Carex* litter decomposition stages in Bayinbuluk

- alpine wetland during the freeze–thaw period. *Ecol. Indic.* 121, 107180 <https://doi.org/10.1016/j.ecolind.2020.107180>.
- Chernov, T.I., Zhelezova, A.D., Tkhakakhova, A.K., Ksenofontova, N.A., Zverev, A.O., Tiunov, A.V., 2021. Soil microbiome, organic matter content and microbial abundance in forest and forest-derived land cover in Cat Tien National Park (Vietnam). *Appl. Soil Ecol.* 165 (March), 103957 <https://doi.org/10.1016/j.apsoil.2021.103957>.
- Daskalova, G.N., Kamp, J., 2023. Abandoning land transforms biodiversity. *Science* 380 (6645), 581–583. <https://doi.org/10.1126/science.adf1099>.
- De Cáceres, M., Legendre, P., 2009. Associations between species and groups of sites: indices and statistical inference. *Ecology* 90 (12), 3566–3574. <https://doi.org/10.1890/08-1823.1>.
- Delgado-Baquerizo, M., Oliverio, A.M., Brewer, T.E., Benavent-González, A., Eldridge, D. J., Bardgett, R.D., Maestre, F.T., Singh, B.K., Fierer, N., 2018. A global atlas of the dominant bacteria found in soil. *Science* 359 (6373), 320–325. <https://doi.org/10.1126/science.aap9516>.
- Dixon, P., 2003. VEGAN, a package of R functions for community ecology. *J. Veg. Sci.* 14 (6), 927–930. [https://doi.org/10.1658/1100-9233\(2003\)014\[0927:vaporf\]2.0.co;2](https://doi.org/10.1658/1100-9233(2003)014[0927:vaporf]2.0.co;2).
- Douglas, G.M., Maffei, V.J., Zanevel, J.R., Yurgel, S.N., Brown, J.R., Taylor, C.M., Huttenhower, C., Langille, M.G.L., 2020. PICRUST2 for prediction of metagenome functions. *Nat. Biotechnol.* 38, 685–688. <https://doi.org/10.1038/s41587-020-0548-6>.
- Enchilik, P.R., Klink, G.V., Peunova, A.A., Prilipova, E.S., Sergeeva, E.A., Sobolev, N.S., Semenov, I.N., 2023. Postagrogenic dynamics of pH, electrical conductivity and redox potential in soils of diverse texture at the Smolensk Poozerie National Park (Russia). *Vestnik Tomskogo Gosudarstvennogo Universiteta. Biologiya = Tomsk State University. J. Biol.* 64, 6–29. <https://doi.org/10.17223/19988591/64/1>.
- Fernandes, A.D., Reid, J.N.S., Macklaim, J.M., McMurrough, T.A., Edgell, D.R., Gloor, G. B., 2014. Unifying the analysis of high-throughput sequencing datasets: characterizing RNA-seq, 16S rRNA gene sequencing and selective growth experiments by compositional data analysis. *Microbiome* 2 (1), 1–13. <https://doi.org/10.1186/2049-2618-2-15>.
- Gajare, S., Divatar, M., Ahmed, S., Shivalee, A., Kattimani, L., 2016. Exploration of potent soil bacteria for Menaquinone-7 production ISSN 2277–3843 Original Article Exploration of potent soil bacteria for Menaquinone-7 production, 6(June), pp. 3–7.
- Gao, H., Ren, A., Zhang, S., Yuan, L., 2023. Soil bacterial diversity and its influencing factors of walnut forests with different stand ages in Xizang Plateau of northwestern China. *Beijing Linye Daxue Xuebao/Journal of Beijing Forestry University* 45 (11), 100–109. <https://doi.org/10.12171/j.1000-1522.20230051>.
- Gloor, G.B., Macklaim, J.M., Fernandes, A.D., 2016. Displaying variation in large datasets: plotting a visual summary of effect sizes. *J. Comput. Graph. Stat.* 25 (3), 971–979. <https://doi.org/10.1080/10618600.2015.1131161>.
- Górska, E.B., Stepien, W., Hewelke, E., Lata, J.-C., Gworek, B., Gozdowski, D., Sas-Pasz, L., Bazot, S., Lisek, A., Gradowski, M., Baczewska-Dąbrowska, A.H., Dobrzyński, J., 2024. Response of soil microbiota to various soil management practices in 100-year-old agriculture field and identification of potential bacterial ecological indicator. *Ecol. Indic.* 158, 111545 <https://doi.org/10.1016/j.ecolind.2024.111545>.
- Gschwend, P., Hartmann, M., Mayerhofer, J., Hug, A.S., Enkerli, J., Gubler, A., Meuli, R. G., Frey, B., Widmer, F., 2022. Site and land-use associations of soil bacteria and fungi define core and indicative taxa. *FEMS Microbiol. Ecol.* 97 (12), 1–14. <https://doi.org/10.1093/femsec/fiab165>.
- Gunina, A., Kuz'yakov, Y., 2015. Sugars in soil and sweets for microorganisms: review of origin, content, composition and fate. *Soil Biol. Biochem.* 90, 87–100. <https://doi.org/10.1016/j.soilbio.2015.07.021>.
- Hermans, S.M., Taylor, M., Grelet, G., Curran-Cournane, F., Buckley, H.L., Handley, K. M., Lear, G., 2020. From pine to pasture: land use history has long-term impacts on soil bacterial community composition and functional potential. *FEMS Microbiol. Ecol.* 96 (4), f1aa041. <https://doi.org/10.1093/femsec/f1aa041>.
- Ignatov, M.S., Afonina, O.M., Ignatova, E.A., Abolina, A.A., Akatova, T.V., Baisheva, E.Z., Bardunov, L.V., Baryakina, E.A., Belkina, O.A., Bezgodov, A.G., Boychuk, M.A., Cherdantseva, V.Ya., Czernyjadjeva, I.V., Doroshina, G.Ya., Dyachenko, A.P., Fedosov, V.E., Goldberg, I.L., Ivanova, E.I., Jukoniene, I., Zolotov, V.I., 2006. Checklist of mosses of East Europe and North Asia. *Arctoa*. <https://doi.org/10.15298/arctoa.15.01>.
- Islam, W., Saqib, H.S.A., Adnan, M., Wang, Z., Tayyab, M., Huang, Z., Chen, H.Y.H., 2022. Differential response of soil microbial and animal communities along the chronosequence of *Cunninghamia lanceolata* at different soil depth levels in subtropical forest ecosystem. *J. Adv. Res.* 38, 41–54. <https://doi.org/10.1016/j.jare.2021.08.005>.
- IUSS Working Group WRB, 2022. World Reference Base for Soil Resources. International Soil Classification System for Naming Soils and Creating Legends for Soil Maps, 4th editio. International Union of Soil Sciences.
- Ivanova, E.A., Pershina, E.V., Shapkin, V.M., Kichko, A.A., Aksenova, T.S., Kimeklis, A. K., Gladkov, G.V., Zverev, A.O., Vasilyeva, N.A., Andronov, E.E., Abakumov, E.V., 2020. Shifting prokaryotic communities along a soil formation chronosequence and across soil horizons in a South Taiga ecosystem. *Pedobiologia* 81–82, 150650. <https://doi.org/10.1016/j.pedobi.2020.150650>.
- Jones, D.L., 1999. Amino acid biodegradation and its potential effects on organic nitrogen capture by plants. *Soil Biol. Biochem.* 31 (4), 613–622. [https://doi.org/10.1016/S0038-0717\(98\)00167-9](https://doi.org/10.1016/S0038-0717(98)00167-9).
- Kaiser, K., Wemheuer, B., Korolkow, V., Wemheuer, F., Nacke, H., Schöning, I., Schrupp, M., Daniel, R., 2016. Driving forces of soil bacterial community structure, diversity, and function in temperate grasslands and forests. *Sci. Rep.* 6 (1), 33696. <https://doi.org/10.1038/srep33696>.
- Kang, M.-J., Baek, K.-R., Lee, Y.-R., Kim, G.-H., Seo, S.-O., 2022. Production of vitamin K by wild-type and engineered microorganisms. *Microorganisms* 10 (3), 554. <https://doi.org/10.3390/microorganisms10030554>.
- Kassambara, A., 2020. Ggpubr. R Package Version 0.4.0.
- Katoh, K., Standley, D.M., 2013. MAFFT multiple sequence alignment software version 7: improvements in performance and usability. *Mol. Biol. Evol.* 30 (4), 772–780. <https://doi.org/10.1093/molbev/mst010>.
- Kemmitt, S.J., Wright, D., Murphy, D.V., Jones, D.L., 2008. Regulation of amino acid biodegradation in soil as affected by depth. *Biol. Fertil. Soils* 44 (7), 933–941. <https://doi.org/10.1007/s00374-008-0278-2>.
- Kim, G., Bae, J., Kim, M.J., Kwon, H., Park, G., Kim, S.J., Choe, Y.H., Kim, J., Park, S.H., Choe, B.H., Shin, H., Kang, B., Magoč, T., Salzberg, S.L., Quast, C., Pruesse, E., Yilmaz, P., Gerken, J., Schweer, T., Armenta, M.A., 2019. The SILVA ribosomal RNA gene database project: improved data processing and web-based tools. *Nucleic Acids Res.* 41 (D1), D590–D596.
- Kim, H.-S., Lee, S.-H., Jo, H.Y., Finneran, K.T., Kwon, M.J., 2021. Diversity and composition of soil Acidobacteria and Proteobacteria communities as a bacterial indicator of past land-use change from forest to farmland. *Sci. Total Environ.* 797, 148944 <https://doi.org/10.1016/j.scitotenv.2021.148944>.
- Kolb, S., 2009. Aerobic methanol-oxidizing Bacteria in soil. *FEMS Microbiol. Lett.* 300 (1), 1–10. <https://doi.org/10.1111/j.1574-6968.2009.01681.x>.
- Kuhn, M., Wing, J., Weston, S., Williams, A., Keefer, C., Engelhardt, A., Cooper, T., Mayer, Z., Kenkel, B., Benesty, M., Lescarbeau, R., Ziem, A., Scrucca, L., Tang, Y., Candan, C., Hunt, T., 2023. Caret: classification and regression training. R Core Team. <https://doi.org/10.32614/CRAN.package.caret>.
- Kuroshima, T., Hayano, K., 1982. Phospholipase C activity in soil. *Soil Sci. Plant Nutr.* 28 (4), 535–542. <https://doi.org/10.1080/00380768.1982.10432393>.
- Lan, J., Wang, S., Wang, J., Qi, X., Long, Q., Huang, M., 2022. The shift of soil bacterial community after afforestation influence soil organic carbon and aggregate stability in Karst Region. *Front. Microbiol.* 13, 901126 <https://doi.org/10.3389/fmicb.2022.901126>.
- Lavrishchev, A., Litvinovich, A., Abakumov, E., Kimeklis, A., Gladkov, G., Andronov, E., Polyakov, V., 2024. Soil microbiome of abandoned Plaggic Podzol of different-aged fallow lands and native Podzol in South Taiga (Leningrad region). *Agronomy* 14 (3), 429. <https://doi.org/10.3390/agronomy14030429>.
- Liu, Y., Wang, C., Zhang, T., Ye, C., Chu, X., Liao, W., Li, R., Wu, Y., 2024. Bacterial diversity exploring and functional prediction in ancient rice original-producing region of Wannian County, China*. *Chin. J. Eco-Agric.* 32 (3), 380–390. <https://doi.org/10.12357/cjca.20230448>.
- Lu, Q., Jiang, Z., Peng, W., Yu, C., Jiang, F., Huang, J., Cui, J., 2023. Exploration of bacterial community-induced polycyclic aromatic hydrocarbons degradation and humus formation during co-composting of cow manure waste combined with contaminated soil. *J. Environ. Manage.* 326, 116852 <https://doi.org/10.1016/j.jenvman.2022.116852>.
- Luo, J., Tillman, R.W., White, R.E., Ball, P.R., 1998. Variation in denitrification activity with soil depth under pasture. *Soil Biol. Biochem.* 30 (7), 897–903. [https://doi.org/10.1016/S0038-0717\(97\)00206-X](https://doi.org/10.1016/S0038-0717(97)00206-X).
- Lyuri, D.I., Goryachkin, S.V., Karavaeva, N.A., Denisenko, E.A., Nefedova, T.G., 2010. Dynamics of Agricultural Lands of Russia in XX Century and Postagrogenic Restoration of Vegetation and Soils. GEOS.
- Maevs'kii, P.F., 2014. In: Novikov, V.S., Pavlov, V.N., Sokoloff, D.D., Timonin, A.K., Alekseev, Yu E., Maiorov, S.R. (Eds.), Flora of the middle zone of the European part of Russia. *Tovarishchestvo Nauchnykh Izdaniy KMK*.
- McMurdie, P.J., Holmes, S., 2013. PhyloSeq: An R package for reproducible interactive analysis and graphics of microbiome census data. *PLoS One* 8 (4), e61217. <https://doi.org/10.1371/journal.pone.0061217>.
- Merloti, L.F., Mendes, L.W., Pedrinho, A., de Souza, L.F., Ferrari, B.M., Tsai, S.M., 2019. Forest-to-agriculture conversion in Amazon drives soil microbial communities and N-cycle. *Soil Biol. Biochem.* 137, 107567 <https://doi.org/10.1016/j.soilbio.2019.107567>.
- Morigasaki, S., Matsui, M., Ohtsu, I., Doi, Y., Kawano, Y., Nakai, R., Iwasaki, W., Hayashi, H., Takaya, N., 2024. Temporal and fertilizer-dependent dynamics of soil bacterial communities in buckwheat fields under long-term management. *Sci. Rep.* 14 (1), 9896. <https://doi.org/10.1038/s41598-024-60655-w>.
- Muhammad, I., Yang, L., Ahmad, S., Zeeshan, M., Farooq, S., Ali, I., Khan, A., Zhou, X.B., 2022. Irrigation and nitrogen fertilization alter soil bacterial communities, soil enzyme activities, and nutrient availability in maize crop. *Front. Microbiol.* 13, 833758 <https://doi.org/10.3389/fmicb.2022.833758>.
- Pansu, M., Gautheyrou, J., 2006. Handbook of soil analysis. In: *Handbook of Soil Analysis*. <https://doi.org/10.1007/978-3-540-31211-6>.
- Pershina, E.V., Ivanova, E.A., Korvigo, I.O., Chirak, E.L., Sergaliev, N.H., Abakumov, E. V., Provorov, N.A., Andronov, E.E., 2018. Investigation of the core microbiome in main soil types from the east European plain. *Sci. Total Environ.* 631–632, 1421–1430. <https://doi.org/10.1016/j.scitotenv.2018.03.136>.
- Pressler, Y., Zhou, J., He, Z., Van Nostrand, J.D., Smith, A.P., 2020. Post-agricultural tropical forest regeneration shifts soil microbial functional potential for carbon and nutrient cycling. *Soil Biol. Biochem.* 145, 107784 <https://doi.org/10.1016/j.soilbio.2020.107784>.
- Price, M.N., Dehal, P.S., Arkin, A.P., 2010. FastTree 2—approximately maximum-likelihood trees for large alignments. *PLoS One* 5 (3), e9490. <https://doi.org/10.1371/journal.pone.0009490>.
- Qi, D., Feng, F., Fu, Y., Ji, X., Liu, X., 2020. Effects of soil microbes on forest recovery to climax community through the regulation of nitrogen cycling. *Forests* 11 (10), 1027. <https://doi.org/10.3390/f11101027>.

- Qu, Z.L., Liu, B., Ma, Y., Xu, J., Sun, H., 2020. The response of the soil bacterial community and function to forest succession caused by forest disease. *Funct. Ecol.* 34 (12), 2548–2559. <https://doi.org/10.1111/1365-2435.13665>.
- van Reeuwijk, L.P., 2002. Procedures for soil analysis. In: Reeuwijk, L.P. (Ed.), *International Soil Reference and Information Centre (Third Edit)*. ISRIC FAO.
- Robeson, M.S., O'Rourke, D.R., Kaehler, B.D., Ziemski, M., Dillon, M.R., Foster, J.T., Bokulich, N.A., 2021. RESCRIP: reproducible sequence taxonomy reference database management. *PLoS Comput. Biol.* 17 (11), e1009581 <https://doi.org/10.1371/journal.pcbi.1009581>.
- Semenkov, I.N., Shelyakin, P.V., Nikolaeva, D.D., Tutukina, M.N., Sharapova, A.V., Lednev, S.A., Sarana, Y.V., Gelfand, M.S., Krechetov, P.P., Koroleva, T.V., 2023. Data on the temporal changes in soil properties and microbiome composition after a jet-fuel contamination during the pot and field experiments. *Data Brief* 46, 108860. <https://doi.org/10.1016/j.dib.2022.108860>.
- Semenov, M.V., Ksenofontova, N.A., Nikitin, D.A., Tkachkova, A.K., Lukin, S.M., 2023. Microbiological parameters of Soddy-Podzolic soil and its rhizosphere in a half-century field experiment with different fertilizer systems. *Eurasian Soil Sci.* 56 (6), 756–768. <https://doi.org/10.1134/S1064229323600070>.
- Shang, C., Chen, A., Cao, R., Luo, S., Shao, J., Zhang, J., Peng, L., Huang, H., 2023. Response of microbial community to the remediation of neonicotinoid insecticide imidacloprid contaminated wetland soil by *Phanerochaete chrysosporium*. *Chemosphere* 311, 136975. <https://doi.org/10.1016/j.chemosphere.2022.136975>.
- Shao, P., Liang, C., Rubert-Nason, K., Li, X., Xie, H., Bao, X., 2019. Secondary successional forests undergo tightly-coupled changes in soil microbial community structure and soil organic matter. *Soil Biol. Biochem.* 128, 56–65. <https://doi.org/10.1016/j.soilbio.2018.10.004>.
- Shelyakin, P.V., Semenov, I.N., Tutukina, M.N., Nikolaeva, D.D., Sharapova, A.V., Sarana, Y.V., Lednev, S.A., Smolenkov, A.D., Gelfand, M.S., Krechetov, P.P., Koroleva, T.V., 2022. The influence of kerosene on microbiomes of diverse soils. *Life* 12 (2), 221. <https://doi.org/10.3390/life12020221>.
- Sheremet, A., Jones, G.M., Jarett, J., Bowers, R.M., Bedard, I., Culham, C., Eloe-Fadrosch, E.A., Ivanova, N., Malmstrom, R.R., Grasby, S.E., Woyke, T., Dunfield, P.F., 2020. Ecological and genomic analyses of candidate phylum WPS-2 bacteria in an unvegetated soil. *Environ. Microbiol.* 22 (8), 3143–3157. <https://doi.org/10.1111/1462-2920.15054>.
- Shopina, O.V., Geraskina, A.P., Kuznetsova, A.I., Tikhonova, E.V., Titovets, A.V., Bavshin, I.M., Khokhryakov, V.R., Semenov, I.N., 2023. Stages of restoration of the components of postagrogenic pine forest ecosystems in the Smolenskoye Poozerye National Park. *Eurasian Soil Sci.* 56 (1), 16–28. <https://doi.org/10.1134/S1064229322601639>.
- Song, D., Zhao, W., Li, G., Wang, L., Ma, R., Ren, H., Wu, H., 2024. Effects of abandoned farmland on key microorganisms and functional genes of soil carbon and nitrogen cycles in Minqin Oasis. *Shengtai Xuebao*. <https://doi.org/10.20103/j.stxb.202211013107>.
- Stavridou, E., Giannakis, I., Karamichali, I., Kamou, N.N., Lagiotis, G., Madesis, P., Emmanouil, C., Kungolos, A., Naniou-Obeidat, I., Lagopodi, A.L., 2021. Biosolid-amended soil enhances defense responses in tomato based on metagenomic profile and expression of pathogenesis-related genes. *Plants* 10 (12), 2789. <https://doi.org/10.3390/plants10122789>.
- Tang, K.H., Tang, Y.J., Blankenship, R.E., 2011. Carbon metabolic pathways in phototrophic bacteria and their broader evolutionary implications. *Front. Microbiol.* 2 (AUG) <https://doi.org/10.3389/FMICB.2011.00165>.
- Terekhova, D.A., Smirnova, M.A., Geraskina, A.P., Shopina, O.V., Kuznetsova, A.I., Bavshin, I.M., Klink, G.V., Enchilik, P.R., Khokhryakov, V.R., Gerasimova, M.I., Semenov, I.N., 2023. Macrofauna and organic matter in postagrogenic sandy soils in the northwest of Smolensk oblast (Russia). *Eurasian Soil Sci.* 56 (8), 1139–1151. <https://doi.org/10.1134/S1064229323600902>.
- Trentini, C.P., Campanello, P.I., Villagra, M., Ferreras, J., Hartmann, M., 2020. Thinning partially mitigates the impact of Atlantic Forest replacement by pine monocultures on the soil microbiome. *Front. Microbiol.* 11 (July), 1–18. <https://doi.org/10.3389/fmicb.2020.01491>.
- Tripathi, B.M., Kim, H.M., Jung, J.Y., Nam, S., Hyeon Tae, Ju, Kim, M., Lee, Y.K., 2019. Distinct taxonomic and functional profiles of the microbiome associated with different soil horizons of a moist tussock tundra in Alaska. *Front. Microbiol.* 10 (JUN), 1442. <https://doi.org/10.3389/fmicb.2019.01442>.
- Turner, S., Mikutta, R., Meyer-Stüve, S., Guggenberger, G., Schaarschmidt, F., Lazar, C.S., Dohrmann, R., Schippers, A., 2017. Microbial community dynamics in soil depth profiles over 120,000 years of ecosystem development. *Front. Microbiol.* 8 (MAY), 1–17. <https://doi.org/10.3389/fmicb.2017.00874>.
- Wang, G., Liu, Y., Cui, M., Zhou, Z., Zhang, Q., Li, Y., Ha, W., Pang, D., Luo, J., Zhou, J., 2022. Effects of secondary succession on soil fungal and bacterial compositions and diversities in a karst area. *Plant and Soil* 475 (1–2), 91–102. <https://doi.org/10.1007/s11104-021-05016-6>.
- Wu, L., Ren, C., Jiang, H., Zhang, W., Chen, N., Zhao, X., Wei, G., Shu, D., 2024. Land abandonment transforms soil microbiome stability and functional profiles in apple orchards of the Chinese Losses Plateau. *Sci. Total Environ.* 906, 167556. <https://doi.org/10.1016/j.scitotenv.2023.167556>.
- Xu, Y., Jeanne, T., Hogue, R., Shi, Y., Ziadi, N., Parent, L.E., 2021. Soil bacterial diversity related to soil compaction and aggregates sizes in potato cropping systems. *Applied Soil Ecology* 168 (December 2020), 104147. <https://doi.org/10.1016/j.apsoil.2021.104147>.
- Yang, W., Cai, X., Wang, Y., Diao, L., Xia, L., An, S., Luo, Y., Cheng, X., 2022. Increased soil bacterial abundance but decreased bacterial diversity and shifted bacterial community composition following secondary succession of old-field. *Forests* 13 (10), 1628. <https://doi.org/10.3390/f13101628>.
- Zhang, Z., Zhang, L., Zhang, L., Chu, H., Zhou, J., Ju, F., 2024. Diversity and distribution of biosynthetic gene clusters in agricultural soil microbiomes. *mSystems* 9 (4). <https://doi.org/10.1128/msystems.01263-23>, 01263–23.
- Zheng, B., Xiao, Z., Liu, J., Zhu, Y., Shuai, K., Chen, X., Liu, Y., Hu, R., Peng, G., Li, J., Hu, Y., Su, Z., Fang, M., Li, J., 2024. Vertical differences in carbon metabolic diversity and dominant flora of soil bacterial communities in farmlands. *Sci. Rep.* 14 (1), 9445. <https://doi.org/10.1038/s41598-024-60142-2>.
- Zhong, R., Wang, P.-R., Sun, P.-J., Lin, W., Ren, A.-X., Ren, Y.-K., Sun, M., Gao, Z.-Q., 2023. Effects of long-term tillage on soil bacterial community structure and physicochemical properties of dryland wheat fields in northern China. *Huan Jing Ke Xue=Huanjing Kexue* 44 (10), 5800–5812. <https://doi.org/10.13227/j.hjxx.202210316>.
- Zhou, Z., Wang, C., Jiang, L., Luo, Y., 2017. Trends in soil microbial communities during secondary succession. *Soil Biol. Biochem.* 115, 92–99. <https://doi.org/10.1016/j.soilbio.2017.08.014>.
- Zhou, T., Wu, S., Pan, H., Lu, X., Du, J., Yang, L., 2023. Heterogeneous habitats in taiga forests with different important values of constructive species changes bacterial beta diversity. *Microorganisms* 11 (10), 2609. <https://doi.org/10.3390/microorganisms11102609>.
- Zverev, A.O., Kichko, A.A., Pinaev, A.G., Provorov, N.A., Andronov, E.E., 2021. Diversity indices of plant communities and their rhizosphere microbiomes: An attempt to find the connection. *Microorganisms* 9 (11), 2339. <https://doi.org/10.3390/microorganisms9112339>.